



Short Communication

Response of heterotrophic nitrifying/aerobic denitrifying strain *Pseudomonas stutzeri* YXH-102 to hypersaline stress [☆]



Younging Wang ^{a,b}, Zhichun Wang ^c, Yangfan Hu ^b, Dexun Zou ^a, Korakot Sombatmankhong ^d, Wen Wang ^{e,*}, Bo Yu ^{b,*}

^a College of Chemical Engineering, Beijing University of Chemical Technology, Beijing, China

^b Department of Microbial Physiological & Metabolic Engineering, State Key Laboratory of Microbial Diversity and Innovative Utilization, Institute of Microbiology, Chinese Academy of Sciences, Beijing, China

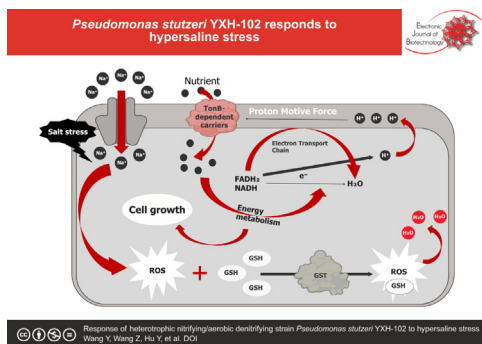
^c Technology Development and Transfer Center, Institute of Microbiology, Chinese Academy of Sciences, Beijing, China

^d National Energy Technology Center, National Science and Technology Development Agency, 114 Thailand Science Park, Khlong Luang, Pathum Thani, Thailand

^e Key Laboratory of Environmental Biotechnology, Research Center for Eco-Environmental Sciences, Chinese Academy of Sciences, Beijing, China

GRAPHICAL ABSTRACT

Response of heterotrophic nitrifying/aerobic denitrifying strain *Pseudomonas stutzeri* YXH-102 to hypersaline stress.



ARTICLE INFO

Article history:

Received 18 March 2025

Accepted 12 May 2025

Available online 2 June 2025

Keywords:

Bioremediation strategies
Comparative transcriptome
Energy metabolism
Heterotrophic nitrification
Hypersaline tolerance
Ion homeostasis
Oxidative stress

ABSTRACT

Background: Hypersaline wastewater poses significant environmental challenges, necessitating efficient bioremediation strategies. This study investigates the hypersaline tolerance mechanisms of *Pseudomonas stutzeri* YXH-102, a heterotrophic nitrifying/aerobic denitrifying bacterium isolated from Yuncheng Salt Lake sediments, under high-salinity stress.

Results: Comparative transcriptomic analysis revealed 268 differentially expressed genes (DEGs) in response to a 10 % NaCl shock, with 86 upregulated and 182 downregulated. Key findings highlight the critical roles of oxidative stress mitigation, energy metabolism adaptation, and ion homeostasis. Salt stress triggered reactive oxygen species (ROS) accumulation, countered by upregulated cytochrome c oxidase (reducing ROS generation) and glutathione S-transferase (enhancing ROS scavenging). Concurrently, energy metabolism pathways, including fatty acid β -oxidation and acetyl-CoA production, were activated to sustain cellular energy demand. Notably, the electron transport chain (ETC) generated a robust proton motive force (PMF), which directly fueled potassium uptake via H^+/K^+ symporters to

[☆] Audio abstract available in Supplementary material.

Peer review under responsibility of Pontificia Universidad Católica de Valparaíso

* Corresponding authors.

E-mail addresses: wenwang@rcees.ac.cn (W. Wang), yub@im.ac.cn (B. Yu).

Pseudomonas stutzeri
ROS
Transcriptomic analysis
Wastewater

counteract osmotic imbalance. TonB-dependent transporters for nutrient uptake were also significantly upregulated, suggesting enhanced nutrient acquisition under salinity.
Conclusions: These findings elucidate how *P. stutzeri* YXH-102 combats salt stress through integrated ROS detoxification, energy optimization, and PMF-driven ion transport, providing molecular insights for its application in hypersaline wastewater bioremediation.

How to cite: Wang Y, Wang Z, Hu Y, et al. Response of heterotrophic nitrifying/aerobic denitrifying strain *Pseudomonas stutzeri* YXH-102 to hypersaline stress. Electron J Biotechnol 2025;76. <https://doi.org/10.1016/j.ejbt.2025.05.001>.

© 2025 The Author(s). Published by Elsevier Inc. on behalf of Pontificia Universidad Católica de Valparaíso. This is an open access article under the CC BY-NC-ND license (<http://creativecommons.org/licenses/by-nc-nd/4.0/>).

1. Introduction

Hypersaline wastewater, generated from industries such as aquaculture, petrochemicals, and textiles, contains elevated concentrations of salts and organic pollutants that threaten ecosystems and human health [1,2,3]. While biological treatment is a cost-effective approach, its efficiency is severely hampered by salt-induced microbial stress, including enzyme inhibition, cytoplasmic lysis, and shifts in microbial community structures [4,5,6]. Although halotolerant bacteria (e.g., *Halomonas* and *Truepera*) have been applied to enhance nitrogen removal in high-salinity systems [7,8,9], their underlying salt tolerance mechanisms remain poorly understood, limiting the rational design of robust bioremediation strategies.

Pseudomonas stutzeri, a model denitrifying bacterium with versatile metabolic capabilities, holds untapped potential for hypersaline wastewater treatment. Notably, certain strains exhibit exceptional adaptability to extreme environments, including nitrogen fixation in saline soils [10] and ammonium removal at low temperatures [11]. Despite its recognized role in nitrogen cycling [12,13,14], the strain responded to acute salt stress, particularly its capacity to balance oxidative stress, energy metabolism, and nutrient transport under osmotic pressure, has not been systematically investigated. This knowledge gap impedes the targeted engineering of high-efficiency strains for the bioremediation of high-salinity wastewater. Here, we isolated *P. stutzeri* strain YXH-102, a halotolerant strain demonstrating dual heterotrophic nitrification and aerobic denitrification (HN/AD) activity. Using comparative transcriptomics, we deciphered its dynamic gene expression profile following a 10% NaCl shock. Our study addresses two critical questions: (1) How does *P. stutzeri* rewire its metabolic networks to counteract salt-induced oxidative damage and energy deficits? (2) What transport systems and osmoregulatory mechanisms enable nutrient acquisition in hypersaline environments? By linking phenotypic resilience (e.g., sustained nitrogen removal) to molecular adaptations, this work provides a mechanistic blueprint for developing biotechnologies tailored to high-salinity wastewater treatment using the strain *P. stutzeri* YXH-102.

2. Materials and methods

2.1. Strain isolation and cultivation conditions

A single colony of *P. stutzeri* YXH-102 was inoculated into either heterotrophic nitrification or denitrification medium and cultured in a temperature-controlled shaker at 30°C and 220 rpm. The heterotrophic nitrification medium contained 0.47 g/L (NH₄)₂SO₄, 2.17 g/L sodium succinate, and 50 mL/L Vogel-Bonner medium E (VBE), which consisted of 5.0 g/L K₂HPO₄, 2.5 g/L MgSO₄·7H₂O, 2.5 g/L NaCl, and 0.05 g/L FeSO₄·7H₂O. In the denitrification medium, KNO₃ (0.72 g/L) was substituted with (NH₄)₂SO₄. For solid medium preparation, 16 g/L agar was added. Cell density (OD₆₀₀)

was measured at different time intervals using a spectrophotometer to monitor the bacterial growth.

2.2. RNA extraction

An overnight culture of *P. stutzeri* YXH-102 was inoculated into 50 mL of fresh medium at an inoculation volume of 1% (v/v). When the optical density at 600 nm (OD₆₀₀) reached approximately 0.55, additional NaCl was added to achieve a final salinity of 10% (w/v). Cells were harvested both before and one hour after the salt shock for RNA extraction, which was performed using the Omega Bio-Tek/E.Z.N.A.® RNA extraction kit. The extracted RNA was subsequently used for transcriptome analysis and quantitative real-time PCR (qRT-PCR) to assess gene expression.

2.3. Transcriptome analysis

To investigate the effects of salt stress and the resistance mechanisms of *P. stutzeri* YXH-102 to salt shock, two sets of RNA-Seq libraries were constructed from the total RNA extracted under salt-shocked and non-salt conditions, respectively. Three biological replicates were applied for comparative transcriptome analysis. Ribosomal (rRNA) was removed by RNA fragmentation, and messenger RNA (mRNA) was reverse-transcribed into complementary DNA (cDNA) using reverse transcriptase to construct the cDNA libraries. Sequencing adapters compatible with the Illumina Nova-Seq platform were ligated to both ends of the cDNA fragments, which were then amplified by PCR and sequenced by AZENTA. Raw sequencing reads were filtered using SeqPrep and Sickle software, yielding high-quality data with Q20 > 97.5 % and Q30 > 93.5 %. RNA-seq data quality assessment and differential gene expression analysis were performed after aligning the reads to reference genomes [15].

2.4. Real-time PCR analysis

The purified total RNA was reverse-transcribed using the PrimeScript™ RT Reagent Kit (Takara, DRR037A) according to the manufacturer's instructions. The TB Green Premix Ex Taq II (Takara) kit was used to prepare the reaction mixture. The ΔΔCT method was applied to calculate the differences in gene expression before and after salt shock, using 16S rRNA as an endogenous control [16]. The primers used for RT-PCR analysis are listed in Table 1.

3. Results and discussion

3.1. Strain isolation and heterotrophic nitrification/aerobic denitrification activity test

Strain YXH-102, isolated from a sediment sample collected at Yuncheng Salt Lake in China, is a heterotrophic nitrifying and aerobic denitrifying bacterium. Based on the alignment of its 16S

Table 1
Primers used for real-time PCR.

Gene	Forward primer	Reverse primer
glutathione S-transferase family protein	5'-ACTGGCGCAGTTGCCTGAA-3'	5'-CCTGGCTGACCGAACAGGA-3'
type III glutamate-ammonia ligase	5'-AGAAGCAGTGGGAGCGTGAG-3'	5'-ATTTTCACAGCCTGCGGGTC-3'
tryptophan synthase subunit alpha	5'-TGGTACTCAACGGCAGCTCC-3'	5'-TCGGTATGGCGCTTGAGGC-3'
tryptophan synthase subunit beta	5'-GAGCTCGCCTACTCCAGC-3'	5'-GTGTGGTTGAGCTTTCGCG-3'
cytochrome-c oxidase cbb3-type subunit II	5'-GGCGAAAGCGTCTACGACC-3'	5'-TTGCGGGGTTGTACAGGTG-3'
cytochrome-c oxidase cbb3-type subunit III	5'-AGAAGCAGTGGGAGCGTGAG-3'	5'-ATTTTCACAGCCTGCGGGTC-3'
bifunctional glutamate N-acetyltransferase/amino-acid acetyltransferase	5'-CGATGCAGACCTCGCCGA-3'	5'-AAGACTGCACTGTTCCCTCC-3'
16S rRNA	5'-AGCCGCGTAATACGAAGGG-3'	5'-AGCTCGCCAGTTTTGGATGC-3'

rRNA gene sequence with reference sequences in the NCBI database, the strain was provisionally identified as *Pseudomonas stutzeri* (data not shown). The growth and heterotrophic nitrification/aerobic denitrification (HN/AD) performance of strain YXH-102 were evaluated using 100 mg/L ammonium nitrogen ($\text{NH}_4^+\text{-N}$) and nitrate nitrogen ($\text{NO}_3^-\text{-N}$) as the sole nitrogen source, respectively. In HN medium, the strain exhibited peak growth with an OD_{600} of 1.2 at 30 h. The accumulation of nitrite nitrogen ($\text{NO}_2^-\text{-N}$) and nitrate nitrogen ($\text{NO}_3^-\text{-N}$) reached their maximum levels at 18 h and 24 h, respectively. After 36 h, the total nitrogen (TN) removal rate reached 95.74% while the $\text{NH}_4^+\text{-N}$ removal rate was 97.34% (Fig. 1a). In AD medium, the maximum OD_{600} of 2.2 was recorded at 24 h, and $\text{NO}_2^-\text{-N}$ accumulation also peaked at this time. The $\text{NO}_3^-\text{-N}$ removal rate reached 98.66% after 36 h (Fig. 1b). The salt tolerance of strain YXH-102 was evaluated by culturing the strain in media supplemented with varying concentrations of NaCl,

and the initial concentration of $\text{OD}_{600} = 0.10$. The cell growth was assessed at the 24-h mark (Fig. 2). These results demonstrated that strain YXH-102 possesses strong HN/AD activity and is capable of withstanding at least 5% (w/v) NaCl.

3.2. Growth curve plotting and determination of the logarithmic phase

The logarithmic phase is a critical period in microbial growth, characterized by high metabolic activity and rapid cell division. During this phase, microorganisms adapt to environmental changes through various molecular mechanisms [17]. For example, the salt-tolerant strain *Citrobacter* sp. exhibits strong physiological activity during the logarithmic phase, alleviating salt stress by secreting extracellular polymers and forming biofilms [18]. Similarly, *E. coli* activates extensive stress response networks during this phase to mitigate oxidation stress [19]. Cells harvested during

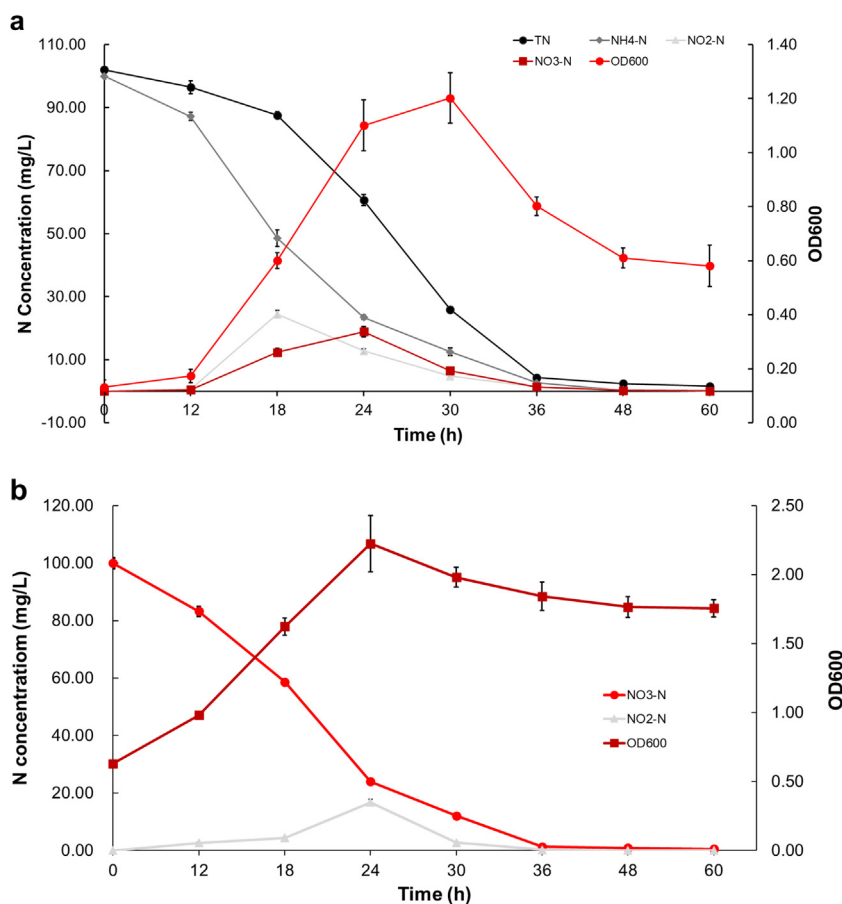


Fig. 1. Cell growth and heterotrophic nitrification/aerobic denitrification activity test of the isolated strain *P. stutzeri* strain YXH-102. (a) Growth and heterotrophic nitrification performance with $\text{NH}_4^+\text{-N}$ as the sole nitrogen source; (b) Growth and aerobic denitrification performance with $\text{NO}_3^-\text{-N}$ as the sole nitrogen source. All the experiments were performed in triplicate. Data shown are mean \pm SD

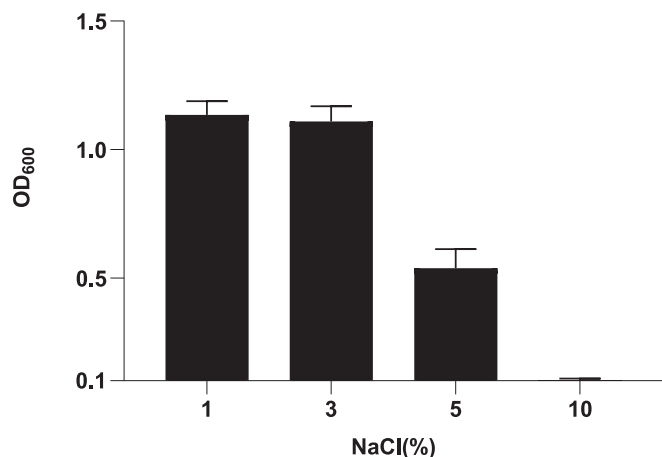


Fig. 2. Salt tolerance of *P. stutzeri* strain YXH-102 with different NaCl addition. The cells were cultivated in LB medium with 1%, 3%, 5% and 10% (w/v) NaCl addition, respectively. The cell density (OD₆₀₀) was measured at the 24-h mark. All the experiments were performed in triplicate. Data shown are mean ± SD.

the logarithmic phase exhibit consistent physiological characteristics, which increases the reliability of experimental data. Therefore, determining the logarithmic phase of *P. stutzeri* is essential for selecting the optimal time point for salt shock experiments and for accurately studying its stress response mechanisms. As shown in Fig. 3a, *P. stutzeri* YXH-102 underwent a prolonged lag phase of approximately 15 h before entering exponential growth, reaching a maximum OD₆₀₀ of 1.30 at 24 h. Based on this growth pattern, cells were subjected to salt shock when the OD₆₀₀ reached approximately 0.55, corresponding to the early exponential phase, when metabolic activity was highest, ensuring reliable transcriptomic results. To investigate the strain's short-term survival mechanisms under lethal salinity stress while avoiding prolonged treatment that could cause massive cell death and ensuring RNA quality suitable for transcriptomic analysis, the bacteria were subjected to 10% NaCl shock, and growth curves were plotted to characterize their physiological status under high-salt conditions (Fig. 3b). The results showed that the cell concentration continued to increase slowly, reaching its peak at approximately 1 h of salt shock, after which it began to gradually decline. Therefore, to simulate hypersaline stress, cells were exposed to a 10% (w/v) NaCl solution for 1 h, even though the strain's growth limit was around 5% NaCl. RNA was then extracted from cells collected both before and after salt shock for subsequent transcriptome analysis.

3.3. Comparative transcriptome analysis of strain YXH-102 under salt shock

A comparative transcriptome approach was employed to examine alterations in gene expression in *P. stutzeri* YXH-102 before and after exposure to salt shock. The samples were designated as group_control and group_treatment, corresponding to non-salt and salt-shock conditions, respectively. After filtering out low-quality reads, 14,918,743 and 14,754,377 clean reads were obtained for group_control and group_treatment. Of these, 87.39% and 88.78% were uniquely aligned to the *P. stutzeri* F2a reference genome (GenBank accession number of AP024722.1). Gene expression levels were quantified using the FPKM (Fragments Per Kilobase of transcript per Million mapped reads) method, calculated with Htseq V0.6.1 software [20]. Differentially expressed genes (DEGs) were identified based on a statistical threshold of p value < 0.05 and a fold change (FC) > 2 or < 0.5. A total of 268 DEGs were detected, including 182 downregulated and 86 upregulated

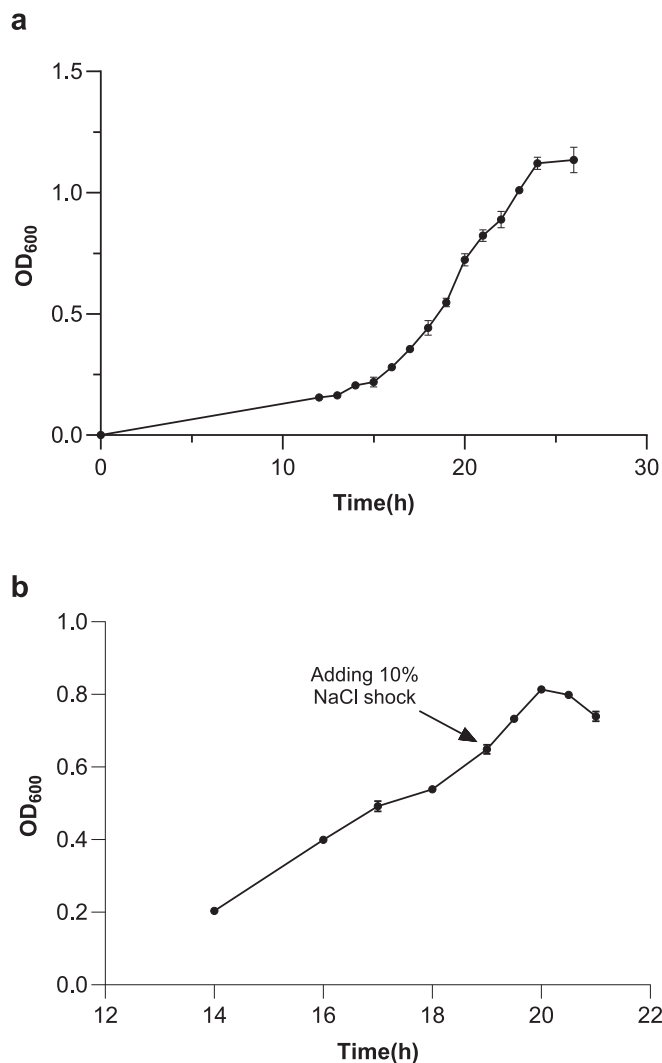


Fig. 3. The cell growth of strain *P. stutzeri* YXH-102. (a) Growth curve of *P. stutzeri* YXH-102 without salt addition for determination of the logarithmic phase; (b) The growth curve of *P. stutzeri* YXH-102 with the addition of 10% NaCl shock after the cell mass value OD₆₀₀ reaching 0.55. All the experiments were performed in triplicate. Data shown are mean ± SD.

genes in the group_treatment compared to group_control. To validate the transcriptome results, seven DEGs were randomly chosen for RT-qPCR analysis under the same experimental conditions. The high consistency between RT-qPCR and RNA-Seq results confirmed the reliability of the transcriptomic data (Table 2). Gene Ontology (GO) functional annotation classified the 268 DEGs into 17 categories: 9 molecular functions, 3 cellular components, and 5 biological processes. These DEGs were mainly associated with the plasma membrane, electron carrier activity, periplasmic space, and heme binding (Fig. 4).

3.4. ROS-mediated oxidative stress poses a major risk under hypersaline conditions

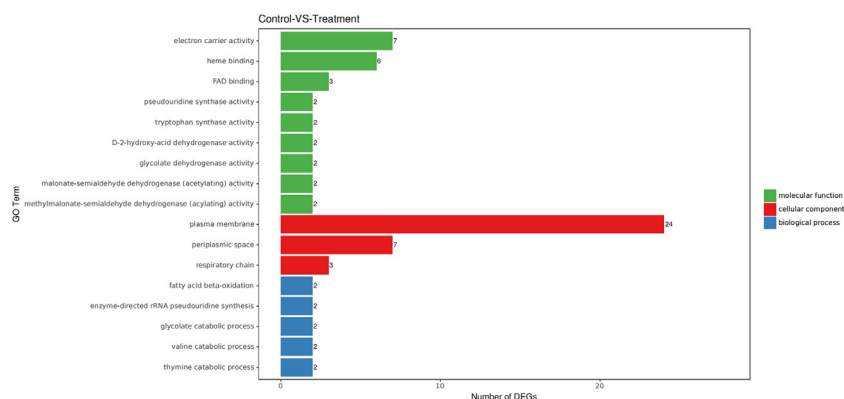
The GO analysis revealed that genes associated with the cell membrane exhibited the most significant expression changes under severe salt stress. This is likely due to oxidative stress induced by salt exposure, which leads to the production of reactive oxygen species (ROS) and damages cellular membranes, thereby affecting the expression of related genes [21]. Moreover, numerous genes related to heme binding were significantly differentially

Table 2

The key gene expression level variations compared by transcriptome (RNA-seq) and RT-PCR analysis validation.

Gene Location [§]	Gene annotation	Fold change by RNA-seq	Fold change by RT-PCR
PszF2a_RS16620	glutathione S-transferase family protein	2.104998	2.329467
PszF2a_RS11470	type III glutamate-ammonia ligase	2.162095	2.86791
PszF2a_RS15010	tryptophan synthase subunit alpha	2.006134	5.426417
PszF2a_RS15005	tryptophan synthase subunit beta	2.17021	2.584706
PszF2a_RS12330	cytochrome-c oxidase cbb3-type subunit II	2.864191	19.15966
PszF2a_RS12335	cytochrome-c oxidase cbb3-type subunit III	2.534583	2.989698
PszF2a_RS16625	bifunctional glutamate N-acetyltransferase/amino-acid acetyltransferase	2.026744	2.514027

[§] The gene names were according to those of strain *P. stutzeri* F2a (GenBank No. AP024722.1), which the reference genome was referenced for this analysis.

**Fig. 4.** GO classification of DEGs in *P. stutzeri* strain YXH-102 under salt stress.

expressed, most of which were downregulated. Previous studies have shown that free heme is extremely toxic and can catalyze the formation of ROS, resulting in cellular damage [22]. Therefore, we hypothesize that the downregulation of heme-binding genes following salt stress may lead to an accumulation of free heme, which in turn promotes excessive ROS production and contributes to oxidative damage. These findings suggest that oxidative stress, driven by ROS accumulation, represents a major threat to *P. stutzeri* YXH-102 under hypersaline conditions.

Furthermore, hypersaline environments disrupt the cellular redox balance, causing ROS accumulation and further cellular injury [23]. Transcriptome analysis showed that the expression levels of cytochrome *c* oxidase and glutathione S-transferase (GST) were significantly upregulated. Previous studies have demonstrated that cytochrome *c* oxidase participates in electron transfer from cytochrome *c* to oxygen, thereby reducing ROS generation [24,25]. Simultaneously, GST facilitates the interaction between ROS and glutathione, enhancing ROS detoxification and clearance [26,27]. Taken together, these results indicate that *P. stutzeri* YXH-102 mitigates oxidative stress in high-salinity environments by both suppressing ROS formation and promoting its removal.

3.5. Energy metabolism plays an important role in the response to salt stress

GO categories related to methylmalonate-semialdehyde dehydrogenase activity (acylating), malonate-semialdehyde dehydrogenase activity (acylating), and fatty acid beta-oxidation were significantly upregulated under salt stress conditions. These enzymes contribute to the generation of acetyl-CoA, a key intermediate in energy metabolism, through acylation and acetylation reactions that catalyze the oxidative decarboxylation of malonic

and methylmalonic aldehydes [28]. Similarly, enhanced fatty acid beta-oxidation facilitates the breakdown of fatty acids, further contributing to acetyl-CoA production. This ensures sufficient energy supply for *P. stutzeri* YXH-102 to maintain metabolic functions under high-salt stress conditions [28]. Collectively, these findings suggest that the upregulation of energy metabolism pathways plays a vital role in the bacterial adaptive response to salt stress.

3.6. Nutrient transport and energy production are critical responses

Annotation results from the Clusters of Orthologous Groups (COG) analysis revealed that the most significantly up-regulated gene transcript changes in *P. stutzeri* YXH-102 under salt stress were predominantly associated with the categories of 'inorganic ion transport and metabolism', 'energy production and conversion', 'amino acid transport and metabolism', 'lipid transport and metabolism', and 'carbohydrate transport and metabolism' (Fig. 5). These findings suggest that nutrient transport and energy production are among the most critical cellular responses in strain YXH-102 when exposed to salt stress.

Transporters, which facilitate the movement of ions and small molecules across cellular membranes, are widely distributed among microorganisms and play a pivotal role in microbial growth and stress resistance [29]. In this study, a total of 13 upregulated transporters were identified, most of which were classified as TonB-dependent carriers. These included three TonB-dependent receptors, four TonB-dependent siderophore receptors, and two additional iron transporters (a FecR domain-containing protein and an imelysin family protein). TonB is a common carrier protein in Gram-negative bacteria that utilizes the proton motive force (PMF) to facilitate the transport of essential nutrients such as iron, vitamin B₁₂, heme, and carbohydrates. This mechanism is particularly important under nutrient- and energy-limited conditions,

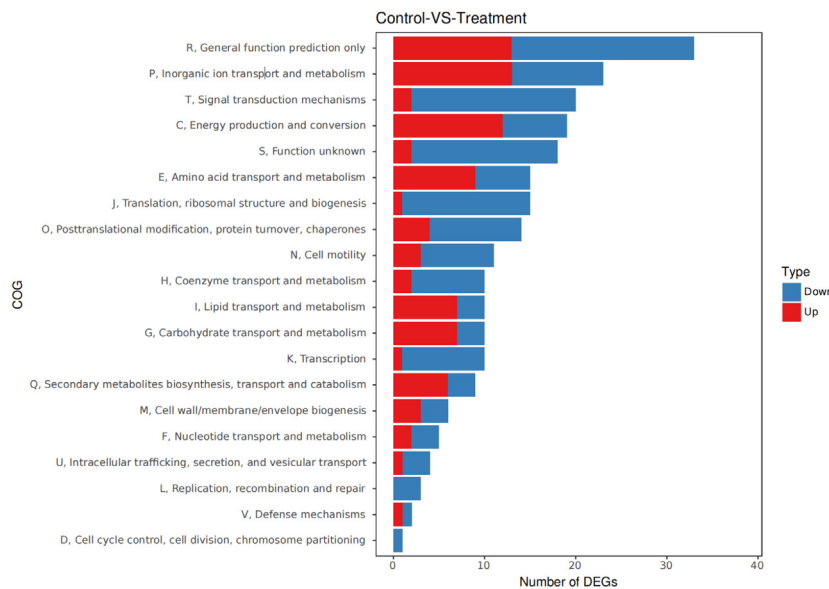


Fig. 5. COG enrichment analysis of differentially expressed genes (DEGs) before and after salt shock treatment on *P. stutzeri* strain YXH-102. The bar chart shows the difference of differentially expressed genes in Clusters of Orthologous Groups of proteins (COG) group in transcriptome data, with the red part representing up-regulated expression and the blue is down-regulated. (For interpretation of the references to color in this figure legend, the reader is referred to the web version of this article).

allowing bacteria to efficiently acquire vital resources required for survival and growth [30,31]. We hypothesize that the upregulation of the TonB system facilitates the import of essential nutrients into microbial cells, supporting cellular adaptation to hypersaline conditions. Notably, PMF generated by the electron transport chain (ETC) is also critical for potassium (K^+) homeostasis through H^+/K^+ symporters such as TrkH family transporters. While TrkH-mediated K^+ uptake is a well-documented osmotic adaptation strategy in bacteria [32], its transcriptional upregulation in *P. stutzeri* YXH-102 under salt stress was not statistically significant. This discrepancy suggests that K^+ transport in this strain may rely on post-transcriptional regulation of existing TrkH proteins or alternative PMF-driven ion transport systems. Further experimental validation, including proteomic analysis and functional assays, is

required to clarify the interplay between PMF, TrkH activity, and osmotic balance in this specific strain. Moreover, the TonB system is an energy-demanding process that relies heavily on PMF generated by the electron transport chain (ETC) [33,34]. This energy requirement may explain the observed downregulation of tRNA synthesis and translation, as the bacterium may be conserving energy by downregulating non-essential metabolic processes in response to salt stress [35].

In summary, under salt stress, the TonB carrier system mediates the active transport of essential nutrients, including vitamin B_{12} and carbohydrates, into the cell, thereby supporting enhanced energy metabolism (Fig. 6). Simultaneously, the increased intracellular sodium concentration caused by salt stress may induce oxidative stress. In response, the upregulation of cytochrome c oxidase

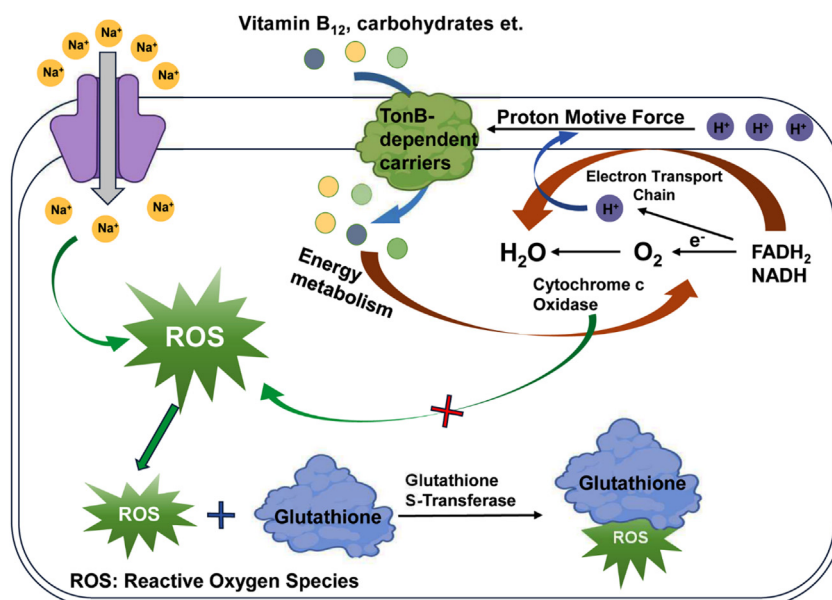


Fig. 6. Schematic diagram of salt-induced changes of important metabolic pathways in *P. stutzeri* strain YXH-102.

helps to reduce ROS, while the elevated expression of glutathione S-transferase (GST) promotes ROS neutralization by enhancing the interaction between glutathione and ROS. Together, these mechanisms help *P. stutzeri* YXH-102 mitigate oxidative damage, maintain cellular function and preserve structural integrity under hypersaline conditions.

4. Conclusions

This study elucidates the potential mechanisms underlying salinity adaptation in the salt-tolerant bacterium *Pseudomonas stutzeri* YXH-102 under hypersaline conditions through a comprehensive analysis of transcriptomic changes pre- and post-salt shock. Specifically, *P. stutzeri* YXH-102 demonstrates resistance to abiotic stress by enhancing nutrient transport and energy metabolism, while mitigating oxidative stress through the upregulation of key enzymes, including cytochrome *c* oxidase and glutathione S-transferase. These findings contribute to a deeper understanding of the genetic basis of salt tolerance in *P. stutzeri* YXH-102 and provide valuable insights into bacterial adaptation to saline environments. Moreover, this work highlights the potential application of *P. stutzeri* YXH-102 in improving the efficiency of bioremediation strategies in high-salinity wastewater treatment systems.

CRediT authorship contribution statement

Younging Wang: Writing – original draft, Investigation. **Zhi-chun Wang:** Resources, Methodology. **Yangfan Hu:** Writing – original draft, Formal analysis. **Dexun Zou:** Formal analysis. **Korakot Sombatmankhong:** Formal analysis, Project administration. **Wen Wang:** Writing – review & editing, Supervision, Data curation. **Bo Yu:** Writing – review & editing, Supervision, Project administration.

Financial support

The work was supported by grants from National Key R&D Program of China (2021YFC2102201), International Partnership Program of Chinese Academy of Sciences (079GJHZ2023026MI), CAS-NSTDA Joint Research Project, Thailand (P2450064) and NSRF via the Program Management Unit for Human Resources & Institutional Development, Research and Innovation, Thailand (B49G680111).

Declaration of competing interest

The authors declared that they had no conflict of interest.

Supplementary material

<https://doi.org/10.1016/j.ejbt.2025.05.001>.

Data availability

Data will be made available on request.

References

- [1] Srivastava A, Parida VK, Majumder A, et al. Treatment of saline wastewater using physicochemical, biological, and hybrid processes: Insights into inhibition mechanisms, treatment efficiencies and performance enhancement. *J Environ Chem Eng* 2021;9(4):105775. <https://doi.org/10.1016/j.jece.2021.105775>.
- [2] Shah A, Arjunan A, Baroutaji A, et al. A review of physicochemical and biological contaminants in drinking water and their impacts on human health. *Water Sci Eng* 2023;16(4):333–44. <https://doi.org/10.1016/j.wse.2023.04.003>.
- [3] Babuji P, Thirumalaisamy S, Duraisamy K, et al. Human health risks due to exposure to water pollution: A review. *Water* 2023;15(14):2532. <https://doi.org/10.3390/w15142532>.
- [4] Ma X, Li Y, Wang L, et al. Hypoxia and salinity constrain the sediment microbiota-mediated N removal potential in an estuary: A multi-trophic interrelationship perspective. *Water Res* 2024;248:120872. <https://doi.org/10.1016/j.watres.2023.120872>. PMID: 38006831.
- [5] Hu N, Li Y, Yin J, et al. A novel *Zobellella endophytica* W14 strain for nitrogen removal from hypersaline wastewater through simultaneous nitrification and denitrification. *J Environ Manage* 2024;371:123171. <https://doi.org/10.1016/j.jenvman.2024.123171>. PMID: 39500170.
- [6] Williams WD. Salinity as a determinant of the structure of biological communities in salt lakes. *Hydrobiologia* 1998;381:191–201. <https://doi.org/10.1023/A:1003287826503>.
- [7] Moussa MS, Sumanasekera DU, Ibrahim SH, et al. Long term effects of salt on activity, population structure and flocc characteristics in enriched bacterial cultures of nitrifiers. *Water Res* 2006;40(7):1377–88. <https://doi.org/10.1016/j.watres.2006.01.029>. PMID: 16530803.
- [8] Yang J, Tian Z, Spanjers H, et al. Feasibility of using NaCl to reduce membrane fouling in anaerobic membrane bioreactors. *Water Environ Res* 2014;86(4):340–5. <https://doi.org/10.2175/106143013X13807328849657>. PMID: 24851330.
- [9] Zhang C, Zhu Y, Li W, et al. Low-carbon and high-ammonia nitrogen dispersed wastewater treatment: From “normal-sludge” to “low-sludge” to “no-sludge” modes. *Environ Res* 2023;233:116498. <https://doi.org/10.1016/j.envres.2023.116498>. PMID: 37356528.
- [10] Chen S, Liu C, Cao G, et al. Effect of salinity on biological nitrogen removal from wastewater and its mechanism. *Environ Sci Pollut Res Int* 2024;31:24713–23. <https://doi.org/10.1007/s11356-024-32417-8>. PMID: 38499924.
- [11] Van Niel CB, Allen MB. A note on *Pseudomonas stutzeri*. *J Bacteriol* 1952;64:413–22. <https://doi.org/10.1128/jb.64.3.413-422.1952>. PMID: 12980914.
- [12] Lalucat J, Bennisar A, Bosch R, et al. Biology of *Pseudomonas stutzeri*. *Microbiol Mol Biol Rev* 2006;70(2):510–47. <https://doi.org/10.1128/MMBR.00047-05>. PMID: 16760312.
- [13] Park SW, Back JH, Lee SW, et al. Successful antibiotic treatment of *Pseudomonas stutzeri*-induced peritonitis without peritoneal dialysis catheter removal in continuous ambulatory peritoneal dialysis. *Kidney Res Clin Pract* 2013;32(2):81–3. <https://doi.org/10.1016/j.krcp.2013.04.004>. PMID: 26877919.
- [14] Fu W-L, Duan P-F, Wang Q, et al. Transcriptomics reveals the effect of ammonia nitrogen concentration on *Pseudomonas stutzeri* F2 assimilation and the analysis of *amtB* function. *Synth Syst Biotechnol* 2023;8(2):262–72. <https://doi.org/10.1016/j.synbio.2023.03.002>. PMID: 37033292.
- [15] Zhang X, Wen H, Wang H, et al. RNA-Seq analysis of salinity stress-responsive transcriptome in the liver of spotted sea bass (*Lateolabrax maculatus*). *PLoS ONE* 2017;12(3):e0173238. <https://doi.org/10.1371/journal.pone.0173238>. PMID: 28253338.
- [16] Dumas J-L, van Delden C, Perron K, et al. Analysis of antibiotic resistance gene expression in *Pseudomonas aeruginosa* by quantitative real-time-PCR. *FEMS Microbiol Lett* 2006;254(2):217–25. <https://doi.org/10.1111/j.1574-6968.2005.00008.x>. PMID: 16445748.
- [17] Ughy B, Nagyapati S, Lajko DB, et al. Reconsidering dogmas about the growth of bacterial populations. *Cells* 2023;12(10):1430. <https://doi.org/10.3390/cells12101430>. PMID: 37408264.
- [18] Chakraborty S, Mondal S. Halotolerant *Citrobacter* sp. remediates salinity stress and promotes the growth of *Vigna radiata* (L) by secreting extracellular polymeric substances (EPS) and biofilm formation: A novel active cell for microbial desalination cell (MDC). *Int Microbiol* 2024;27:291–301. <https://doi.org/10.1007/s10123-023-00386-6>. PMID: 37329438.
- [19] Allen KJ, Griffiths MW. Impact of hydroxyl- and superoxide anion-based oxidative stress on logarithmic and stationary phase *Escherichia coli* O157:H7 stress and virulence gene expression. *Food Microbiol* 2012;29(1):141–7. <https://doi.org/10.1016/j.fm.2011.09.014>. PMID: 22029928.
- [20] Mortazavi A, Williams BA, McCue K, et al. Mapping and quantifying mammalian transcriptomes by RNA-Seq. *Nat Methods* 2008;5:621–8. <https://doi.org/10.1038/nmeth.1226>. PMID: 18516045.
- [21] Sies H, Belousov VV, Chandel NS, et al. Defining roles of specific reactive oxygen species (ROS) in cell biology and physiology. *Nat Rev Mol Cell Biol* 2022;23:499–515. <https://doi.org/10.1038/s41580-022-00456-z>. PMID: 35190722.
- [22] Singh N, Bhatla SC. Nitric oxide and iron modulate heme oxygenase activity as a long distance signaling response to salt stress in sunflower seedling cotyledons. *Nitric Oxide* 2016;53:54–64. <https://doi.org/10.1016/j.niox.2016.01.003>. PMID: 26778276.
- [23] Hasanuzzaman M, Raihan MR, Nowroz F, et al. Insight into the mechanism of salt-induced oxidative stress tolerance in soybean by the application of *Bacillus subtilis*: Coordinated actions of osmoregulation, ion homeostasis, antioxidant defense, and methylglyoxal detoxification. *Antioxidants* 2022;11(10):1856. <https://doi.org/10.3390/antiox11101856>. PMID: 36290578.
- [24] Hill BC. Electron transfer from cytochrome *c* to O₂. *Ann NY Acad Sci* 1988;550(1):98–104. <https://doi.org/10.1111/j.1749-6632.1988.tb35326.x>. PMID: 2854415.
- [25] Ramzan R, Vogt S, Kadenbach B. Stress-mediated generation of deleterious ROS in healthy individuals - role of cytochrome *c* oxidase. *J Mol Med* 2020;98:651–7. <https://doi.org/10.1007/s00109-020-01905-y>. PMID: 32313986.

- [26] Shamsad A, Gautam T, Singh R, et al. Association of mRNA expression and polymorphism of antioxidant glutathione-S-transferase (*GSTM1* and *GSTT1*) genes with the risk of Gestational Diabetes Mellitus (GDM). *Gene* 2024;928:148746. <https://doi.org/10.1016/j.gene.2024.148746>. PMID: 39004322.
- [27] Jena AB, Samal RR, Bhol NK, et al. Cellular Red-Ox system in health and disease: The latest update. *Biomed Pharmacother* 2023;162:114606. <https://doi.org/10.1016/j.biopha.2023.114606>. PMID: 36989716.
- [28] Kedishvili N, Goodwin G, Popov K, et al. Mammalian methylmalonate-semialdehyde dehydrogenase. *Methods Enzymol* 2000;324:207–18. [https://doi.org/10.1016/S0076-6879\(00\)24233-X](https://doi.org/10.1016/S0076-6879(00)24233-X). PMID: 10989432.
- [29] Diallinas G, Martzoukou O. Transporter membrane traffic and function: Lessons from a mould. *FEBS J* 2019;286(24):4861–75. <https://doi.org/10.1111/febs.15078>. PMID: 31583839.
- [30] Tang K, Jiao N, Liu K, et al. Distribution and functions of TonB-dependent transporters in marine bacteria and environments: Implications for dissolved organic matter utilization. *PLOS ONE* 2012;7(7):e41204. <https://doi.org/10.1371/journal.pone.0041204>. PMID: 22829928.
- [31] Samantarrai D, Lakshman Sagar A, Gudla R, et al. TonB-dependent transporters in sphingomonads: Unraveling their distribution and function in environmental adaptation. *Microorganisms* 2020;8(3):359. <https://doi.org/10.3390/microorganisms8030359>. PMID: 32138166.
- [32] Epstein W. The roles and regulation of potassium in bacteria. *Prog Nucleic Acid Res Mol Biol* 2003;75:293–320. [https://doi.org/10.1016/S0079-6603\(03\)75008-9](https://doi.org/10.1016/S0079-6603(03)75008-9). PMID: 14604015.
- [33] Noinaj N, Guillier M, Barnard TJ, et al. TonB-dependent transporters: Regulation, structure, and function. *Annu Rev Microbiol* 2010;4:43–60. <https://doi.org/10.1146/annurev.micro.112408.134247>. PMID: 20420522.
- [34] Ferguson AD, Deisenhofer J. TonB-dependent receptors—Structural perspectives. *Biochimica et Biophysica Acta (BBA) – Biomembranes* 2002;1565(2):318–32. [https://doi.org/10.1016/S0005-2736\(02\)00578-3](https://doi.org/10.1016/S0005-2736(02)00578-3).
- [35] Hernández-Elvira M, Sunnerhagen P. Post-transcriptional regulation during stress. *FEMS Yeast Res* 2022;22(1):foac025. <https://doi.org/10.1093/femsyr/foac025>. PMID: 35561747.